Proceedings of the
Annual Stability Conference
Structural Stability Research Council
San Antonio, Texas, March 19-22, 2024

Stability of open web steel joists with flush frame connections during erection

J. Alex Moore[1], Mark D. Denavit[2]

Abstract

Open web steel joists are highly slender structural members that are susceptible to lateral-torsional buckling before bracing is installed. The stability of joists needs to be properly assessed to ensure safety and efficiency during erection. Current practice for joists is based on a strength equation derived by Minkoff in the 1970s. This equation was derived for the common case of joists with bearing seat connections. Flush frame connections for joists have been recently developed. These connections are similar in form to single-plate shear connections and can provide more restraint than bearing seat connections. With more restraint, less bracing may be required, however, the magnitude of the benefit is unknown. The objective of this research is to quantify the strength of unbraced open web steel joists with flush frame connections and to modify the Minkoff equation to improve its accuracy for joists with flush frame connections. Physical testing of four joists sizes and a variety of connection details, making up 60 different configurations, was conducted. The joists with flush frame connections supported more load than the joists of the same designation with bearing seat connections in almost all cases. Based on the experimental results, a modification to the Minkoff equation, specifically a new effective length factor for joists with flush frame connections, is proposed. The proposed modification will enable engineers to preserve the efficiency of open web steel joists while also ensuring safety during erection.

1. Introduction

Open web steel joists are efficient and economical structural members. Their efficiency is achieved, in part, through judicious use of bracing, which allows these relatively slender members to be designed near their plastic capacity. Bracing, also referred to as bridging, is required for the permanent condition and during construction, and may be required during erection. Erection bridging is required when a joist is not stable under its own self-weight and the weight of one erector. Special rules apply to joists on column lines which may be subjected to axial compression. Joists not on a column line are typically not subject to significant axial forces during erection; however, bridging may still be required for these members since they are susceptible to lateral-torsional buckling.

[1] Graduate Research Assistant, University of Tennessee, Knoxville, <mjx356@vols.utk.edu>
[2] Associate Professor, University of Tennessee, Knoxville, <mdenavit@utk.edu>

Requirements for erection bridging are included in SJI *Specifications* (2020) Section 5.5.2.1. For joist spans 60 ft or less in length, bolted diagonal erection bridging is required if the entry for the joist is shaded red in the SJI Load Tables. For these joists, the row of bridging nearest the midspan must be diagonal bridging with bolted connections at chords and intersections and hoisting cables must not be released until this row of bridging is completely installed. If the joist is not in the red shaded area in the SJI Load Tables, then welded horizontal bridging is permitted and this bridging can be installed after the hoisting cables are released. For joist spans greater than 60 ft in length, multiple rows of erection bridging are always required. In the absence of a standard SJI section number designation, erection bridging requirements (for joist spans 60 ft or less in length) can be determined by matching the joist design to an equivalent standard joist or by using the Minkoff equation (SJI *Specifications* (2020) Equation 5.5-1).

Typical open web steel joists have bearing seats that sit atop the supporting member. Joists with flush frame connections have plates at the joist ends that are bolted to plates attached to the supporting members such that the top of the joist is flush with the top of the supporting member. Fig. 1 shows two potential details for flush frame connections of joists to wide flange girders. Flush frame connections can also be made to joist girders.

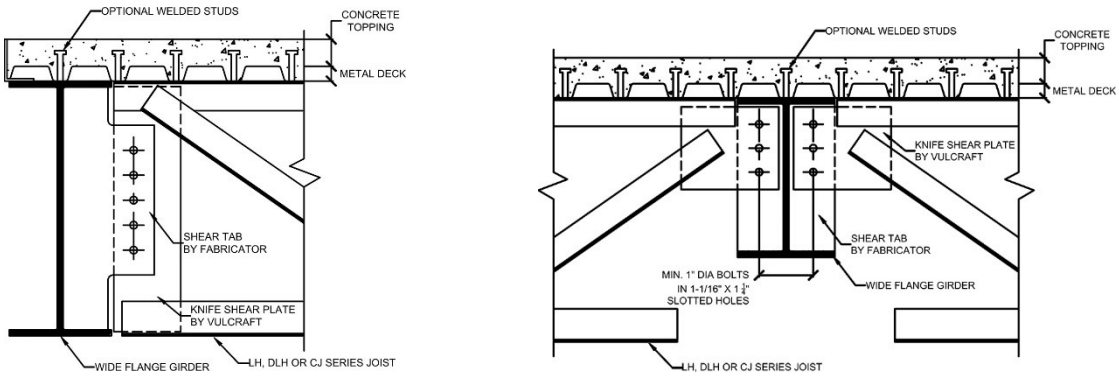

(a) Full-depth connection (b) Top-chord connection

Figure 1: Example flush frame connection details (Vulcraft 2023)

The in-plane rotational stiffness of a flush frame connection is significantly greater than that for a bearing seat connection. Due to the increased connection stiffness and the composite action of the girder made available by the flush framing, floor systems using flush frame connections are more capable of mitigating vibration than traditional joist floor systems (Murray and Davis 2020; Davis and Murray 2022).

The out-of-plane rotational stiffness and torsional stiffness of flush frame connections can also be greater than that of bearing seat connections. These characteristics can help increase resistance to lateral-torsional buckling during erection, potentially leading to less need for erection bridging. The Minkoff equation, used to assess the need for erection bridging, was derived assuming no lateral deflection or twist at the member ends, thus greater torsional stiffness cannot be included in the derivation. However, the benefit of additional out-of-plane rotational stiffness can be expressed through the effective length factor, k, which was not part of the original derivation, but is included in the version of the Minkoff equation included in the SJI *Specifications* (2020).

The objective of this research is to develop design guidance for the erection stability of open web steel joists with flush frame connections. Physical testing of joists without bridging was performed. Experiments consisted of in-plane loading to determine critical loads and out-of-plane loading to determine torsional and rotational stiffnesses. Many configurations of flush frame joists were evaluated with variations in connection plate type, connection plate thickness, and connection eccentricity. The experimental results were compared to results from the Minkoff equation to quantify the accuracy of the Minkoff equation and identify an appropriate effective length factor for use in the equation for joists with flush frame connections. Additional detail of the research, including a description of the out-of-plane bending tests and numerical analyses, are presented elsewhere (Moore and Denavit 2024).

2. Minkoff Equation

Minkoff derived Eq. 1 from the governing differential equation for lateral-torsional buckling using the Rayleigh-Ritz method (Minkoff 1975). The derivation assumed that the joist was a simply supported beam with ends prevented from twist and lateral deflection and that the joist remained elastic. Uniform load acting through the centroid of the cross section (i.e., self-weight) and a point load acting at some height at mid-span (i.e., an erector) were considered.

$$\begin{aligned}&(wL)^2\left(\frac{\pi^2+3}{24}\right)^2+(wL)\left[\left(\frac{\pi^2+3}{12}\right)\left(\frac{P}{16}\right)(\pi^2+4)-\frac{\pi^4 EI_y}{2L^3}\left(\frac{\beta_x(\pi^2-3)}{24}-\frac{y_o}{2}\right)\right]\\&+\left[\frac{P(\pi^2+4)}{16}\right]^2-\frac{\pi^4 EI_y}{2L^3}\left[\frac{\pi^4 EC_w}{2L^3}+\frac{\pi^2 GJ}{2L}+\frac{P\beta_x(\pi^2-4)}{16}-Pa_e\right]=0\end{aligned} \tag{1}$$

where w is the magnitude of the uniform load, L is the joist span, P is the magnitude of the point load, a_e is the vertical location of load P with respect to the shear center (the value of a_e is positive when the point of load application is above the shear center), E is the modulus of elasticity (= 29,000,000 psi for steel), G is the shear modulus (= 11,165,000 psi for steel), I_y is the joist moment of inertia about y-axis, β_x is a cross-sectional parameter, y_o is the distance from the centroid of the cross section to the shear center (the value of y_o is positive when the shear center is below the centroid), C_w is the warping constant, and J is the St. Venant torsion constant.

Equations for the various cross-sectional geometric properties used in the Minkoff equation are presented in the SJI *Specifications* (2020). Key dimensions are shown in Fig. 2.

For use in practice, Eq. 1 can be rewritten as a second-degree polynomial function of $W = wL$ and solved using the quadratic equation as shown in SJI *Specifications* (2020) Section 5.5.2.1. Once the total uniform load that causes buckling, W, is computed, the magnitude of the uniform load that causes buckling, w_u, is computed by dividing by the joist span, $w_u = W/L$. Erection bridging is not required if the joist self-weight is less than w_u. Erection bridging is required if the joist self-weight is greater than or equal to w_u.

The version of the Minkoff equation in SJI *Specifications* (2020) Section 5.5.2.1 was modified from the original Minkoff equation by the addition of an effective length factor, k. In the original derivation, the boundary conditions and deformed shape corresponded to an effective length factor

of k = 1.0 and thus the factor was not included in the original derivation. The SJI *Specifications* (2020) defines the effective length factor, k, equal to 0.85. Galambos (1993) defined the effective length factor as k = 1.00 if the ends of the joist are not welded down and k = 0.85 if one end of the joist is welded down.

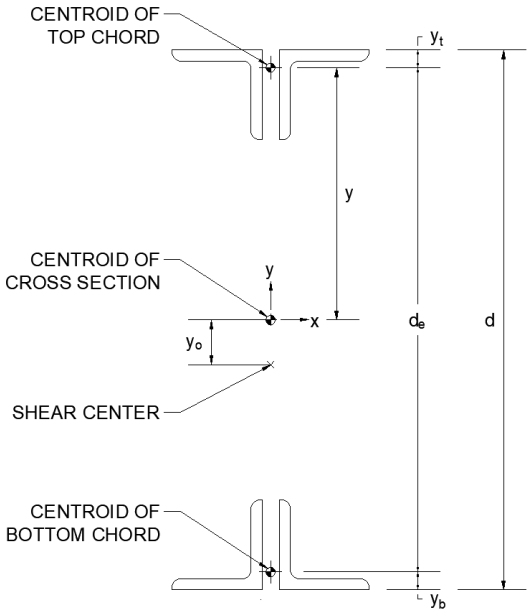

Figure 2: Joist cross section with key dimensions used in the Minkoff equation

The version of the Minkoff equation in SJI *Specifications* (2020) Section 5.5.2.1 is for calculating the uniform load that causes buckling with a given point load. In this research, for comparisons to the experimental results, the opposite was needed: an equation for calculating the point load that causes buckling with a given uniform load. Eq. 1 is also a second-degree polynomial function of P, and thus a derivation similar to that used to derive the version of the equation that appears in the SJI *Specifications* (2020) can be applied to determine the critical value of P. Eq. 2 shows the result of such a derivation and is used in this research to determine the point load that causes buckling with a given uniform load.

$$P = \frac{-b + \sqrt{b^2 - 4ac}}{2a} \tag{2a}$$

$$a = \left(\frac{\pi^2 + 4}{16} \right)^2 \tag{2b}$$

$$b = wL\left(\frac{\pi^2 + 3}{12} \right)\left(\frac{\pi^2 + 4}{16} \right) - \frac{\pi^4 EI_y}{2(kL)^3}\left[\beta_x \left(\frac{\pi^2 - 4}{16} \right) - a_e \right] \tag{2c}$$

$$c = (wL)^2\left(\frac{\pi^2+3}{24}\right)^2 - wL\left(\frac{\pi^4 EI_y}{2(kL)^3}\right)\left[\beta_x\left(\frac{\pi^2-3}{24}\right)-\frac{y_o}{2}\right]-\frac{\pi^4 EI_y}{2(kL)^3}\left(\frac{\pi^4 EC_w}{2(kL)^3}+\frac{\pi^2 GJ}{2kL}\right) \quad (2d)$$

Minkoff presented only limited validation of his eponymous equation but recommended experimental testing to verify its accuracy. Ziemian et al. (2004) described a series of experimental studies to investigate the validity of the Minkoff equation. The tests included a variety of joists ranging from 10 in. to 32 in. deep and a variety of conditions for the bearing connection (e.g., bolts vs. welds and with or without vertical stabilizer plates at the bottom chord). Loads were applied at the top chord at midspan until an out-of-plane deflection of the span divided by 120 was observed. Ziemian et al. (2004) recommended changes to how the Minkoff equation was applied in practice but found it overall to be an accurate and useful analytical tool. However, all the tests performed by Ziemian et al. (2004) had typical bearing seat connections.

3. Methods

Twelve joists were fabricated for this project as listed in Table 1. The twelve consisted of four joist designations, each with one of three end connection types: a bearing seat connection, a full depth flush frame connection, and a top chord flush frame connection. Fig. 3 shows the two types of flush frame joist end connections. The design length was selected to be the same for each of the three joists of the same designation. For the flush frame joists, the design length was defined as centerline of the bolt holes to centerline of the bolt holes. For the bearing seat joists, the design length was defined as the span minus 4 in. (SJI 2020). The span for the flush frame joists is the design length plus the distance from the centerline of the bolt holes to the centerline of the supporting member (i.e., the connection eccentricity) on each end. Since this distance varied from 3 in. to 12 in. among the configurations tested, the joist spans also varied. The span at which erection bridging is required according to the SJI Load Tables is also listed in Table 1. The joist spans were selected to be similar to these limiting values.

Table 1: Joists used in the physical experiments

Name	Joist Designation	End Connection	Design Length	Span at which erection bridging is required	Joist Weight (lbs)
J11	18K3	Bearing Seat	31'-8"	31'	217
J12	18K3	Full Depth Flush Frame	31'-8"	31'	287
J13	18K3	Top Chord Flush Frame	31'-8"	31'	269
J21	30K7	Bearing Seat	43'-8"	44'	373
J22	30K7	Full Depth Flush Frame	43'-8"	44'	569
J23	30K7	Top Chord Flush Frame	43'-8"	44'	431
J31	30K12	Bearing Seat	53'-8"	54'	735
J32	30K12	Full Depth Flush Frame	53'-8"	54'	953
J33	30K12	Top Chord Flush Frame	53'-8"	54'	796
J41	32LH08	Bearing Seat	59'-8"	55'	963
J42	32LH08	Full Depth Flush Frame	59'-8"	55'	1177
J43	32LH08	Top Chord Flush Frame	59'-8"	55'	1013

The weight of each joist was measured with a crane scale and is listed in Table 1. The chord and web members of the flush frame joists were the same as the corresponding bearing seat joist. The larger weight of the flush frame joists is due to the end plates. For the bearing seat joists, the

measured joist weight divided by the design length is close to the approximate joist weight listed in the SJI Load Tables.

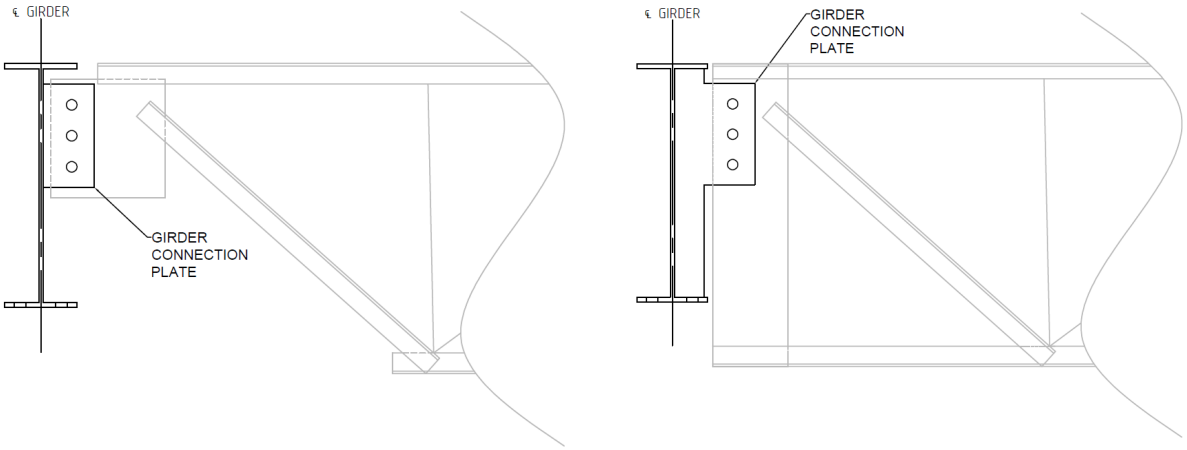

(a) Top chord flush frame connection with tab girder connection plate

(b) Full depth flush frame connection with full depth girder connection plate

Figure 3: End connection plates used in the physical experiments

Dimensions of the chord angles for each joist series are listed in Table 2. The joists were made primarily from rolled angles. All interior web members were single angles that were crimped when the leg length exceeded the chord angle separation. The end diagonals were round or square bar for bearing seat joists J11, J21, and J31 and double angles for bearing seat joist J41 and all the flush frame joists.

Table 2: Chord dimensions

		Joist Series			
Parameter	**Units**	**J1**	**J2**	**J3**	**J4**
Top chord leg length	in.	1.5	2	2	2.5
Top chord leg thickness	in.	0.155	0.137	0.250	0.212
Bottom chord leg length	in.	1.25	1.5	2	2.5
Bottom chord leg thickness	in.	0.133	0.155	0.216	0.212
Angle separation	in.	1	1	1	1

Each bearing seat joist was tested in only one configuration while the flush frame joists were tested in several configurations each. A test matrix outlining the connection configurations is shown in Table 3. There are a total of 15 connection configurations: 1 for the bearing seat joists, 6 for the full depth flush frame joists, and 8 for the top chord flush frame joists. The configurations for the flush frame joists vary in connection eccentricity (i.e., the distance from the centerline of the support to the centerline of the bolt holes), girder connection plate type, and girder connection plate thickness. The girder connection plate was either a tab plate that was only welded to the girder web or a full depth plate that was welded to the girder web and flanges. The two types are shown in Fig. 3. Joists with the full depth flush frame configuration could not be tested with 3 in. connection eccentricity because the joist depth exceeded the flange clearance of the girder.

The 15 connection configurations listed in Table 3 were tested with each of the four joist designations resulting in 60 total configurations. The names of the configurations are denoted Table 3 but with the “X” replaced by a number corresponding to the joist series.

Table 3: Connection configurations

Index	Name	Connection Eccentricity, *a* (in.)	Joist Connection	Joist Connection Plate	Girder Connection Plate Type	Girder Connection Plate Thickness (in.)
1	JX1	n/a	Bearing Seat	n/a	n/a	n/a
2	JX2a	6	Flush Frame	Full Depth	Tab	1/4
3	JX2b	9	Flush Frame	Full Depth	Tab	1/2
4	JX2c	12	Flush Frame	Full Depth	Tab	1/2
5	JX2d	6	Flush Frame	Full Depth	Full Depth	1/4
6	JX2e	9	Flush Frame	Full Depth	Full Depth	1/2
7	JX2f	12	Flush Frame	Full Depth	Full Depth	1/2
8	JX3a	3	Flush Frame	Top Chord	Tab	1/4
9	JX3b	6	Flush Frame	Top Chord	Tab	1/4
10	JX3c	9	Flush Frame	Top Chord	Tab	1/2
11	JX3d	12	Flush Frame	Top Chord	Tab	1/2
12	JX3e	3	Flush Frame	Top Chord	Full Depth	1/4
13	JX3f	6	Flush Frame	Top Chord	Full Depth	1/4
14	JX3g	9	Flush Frame	Top Chord	Full Depth	1/2
15	JX3h	12	Flush Frame	Top Chord	Full Depth	1/2

The flush frame joists fabricated for this project had 1 in. thick connection plates to match the spacing between the chord members. The flush frame connections were made with (3) 1 in. diameter bolts at each end. These bolts were larger than necessary for strength, even if the joists were loaded to their allowable strength. These bolts were used to allow the holes in the joist connection plate to be punched. Standard holes were used in the joist and girder connection plates. The bolts were tightened with a wrench to a snug-tight condition.

The components of the experiment consist of a column assembly, a girder assembly, and safety catches as shown in Fig. 4. The column assembly was secured to the lab's strong floor at either end of the joist and supported the girder assembly. Two safety catches were secured to the strong floor near midspan to keep the joist from deflecting too far and experiencing permanent deformation.

Out-of-plane deflection of the top chord and the bottom chord of the joists was measured using string potentiometers. The string potentiometers were oriented horizontally perpendicular to the joist and attached to the outstanding legs of the chords. The string potentiometer on the bottom chord was located at midspan. The string potentiometer on the top chord was located 4 in. from midspan to avoid the knife edge plate and loading rig at midspan.

For consistency, all flush frame joists were installed such that the direction of the out-of-straightness was towards the girder-side connection plates. Joist out-of-straightness was measured once the joist was installed but before any tests were conducted. A string was pulled above the middle of the top chord at each end. The out-of-straightness was measured at midspan with a measuring tape to the nearest $1/16^{th}$ of an inch.

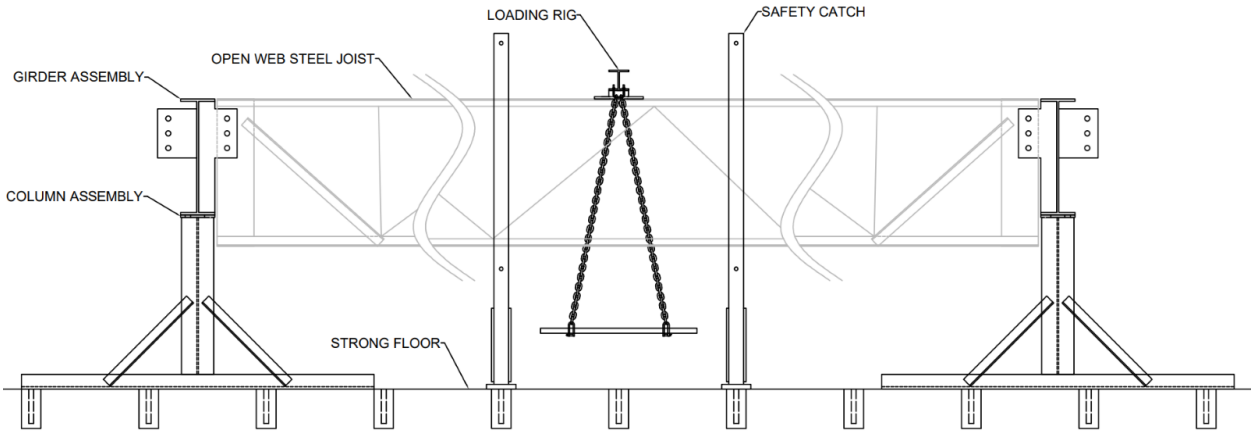

Figure 4: Schematic of in-plane bending experiment

In-plane bending tests were performed to subject the joists to downward vertical load to measure the lateral-torsional buckling strength of the joists. The loading rig was designed to ensure the load was vertical throughout the test. The loading rig was placed at midspan and included a grate to support loading weights under the joist, chains to transfer the load to a spreader beam, and a knife edge support. The knife edge seat plate was bolted to the top chord of the joist. Given the geometry of the knife edge seat, the load was applied 1/2 in. above the top of the top chord. The loading rig and other features of the experiment are shown in Fig. 5.

Before testing, roughly 50 steel angles were weighed on a scale and their weights were written on their surfaces. The steel angle weights were placed by hand on the loading rig. After the placement of each steel angle weight the string potentiometer measurements and the weight written on the angle were recorded. The test was stopped after approximately $L/100$ deflection out-of-plane was achieved, where L is the design length.

The load and deflection data were used to compute two separate critical loads: one based on a deflection limit and another using the Southwell plot method.

The deflection limit load was defined as the load at which the out-of-plane deflection of the top chord at midspan reaches $L/120$, where L is the design length, as shown in Fig. 6. The $L/120$ limit was used in previous studies and is related to the comfort of a erector traversing a joist (Ziemian et al. 2004).

The Southwell plot method was used to quantify the critical buckling load. The plot has top chord deflection on the y axis and top chord deflection divided by applied load on the x axis as shown in Fig. 7. A straight line was fit to the subset of the data with top chord deflection greater than 25% of the maximum recorded top chord deflection. The 25% limit was chosen to exclude the nonlinear region of the plot with relatively low loads and deflections. The slope of the line is the critical buckling load. The Southwell plot method was originally developed for columns but has been shown to apply to beams as well (Mandal and Calladine 2002). The Southwell plot method was used to obtain an experimental estimate of the theoretical elastic buckling strength for structural steel beams undergoing elastic lateral-torsional buckling (Slein et al. 2020).

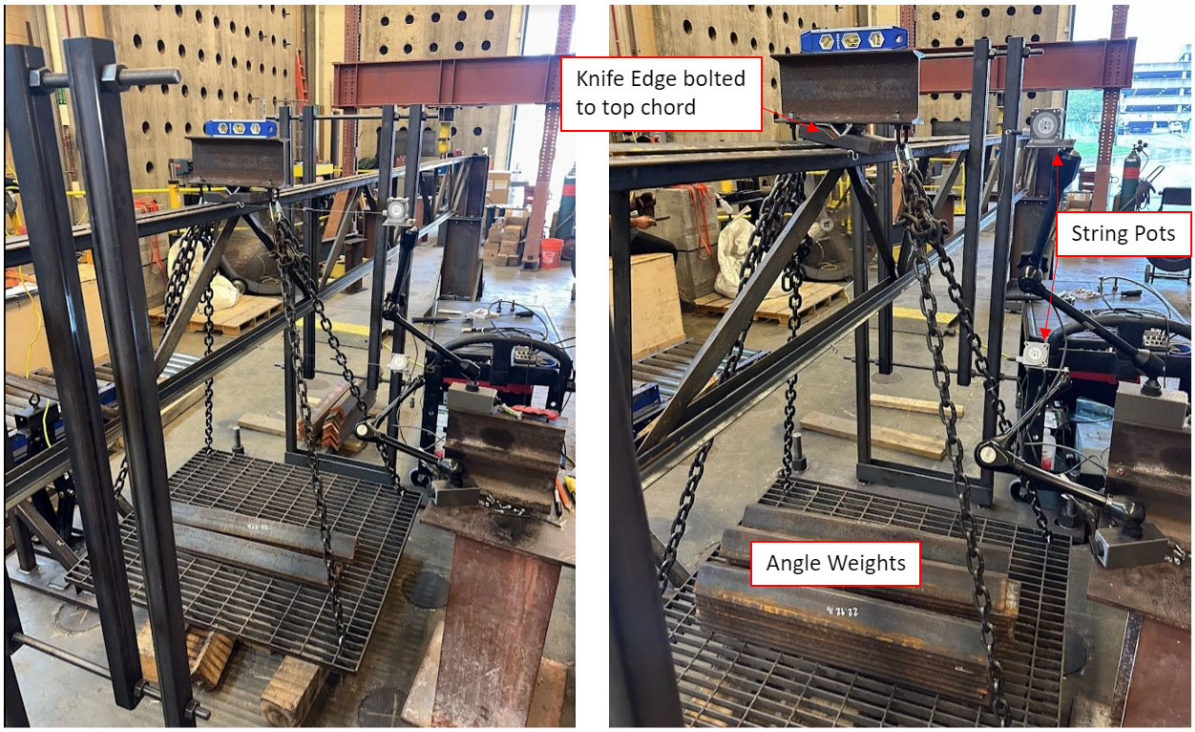

Figure 5: Photographs of in-plane bending experiment

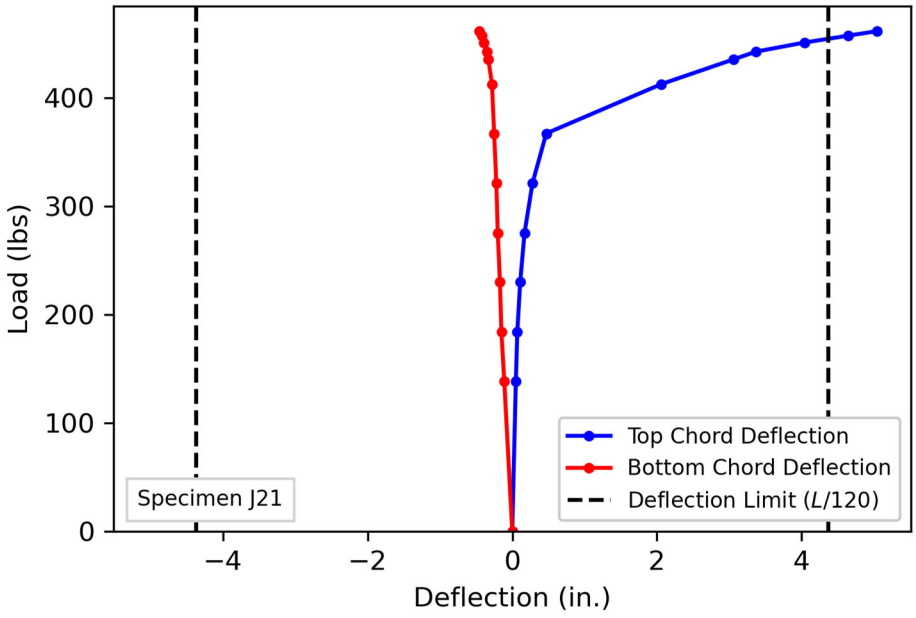

Figure 6: Plot of load vs deflection for example joist

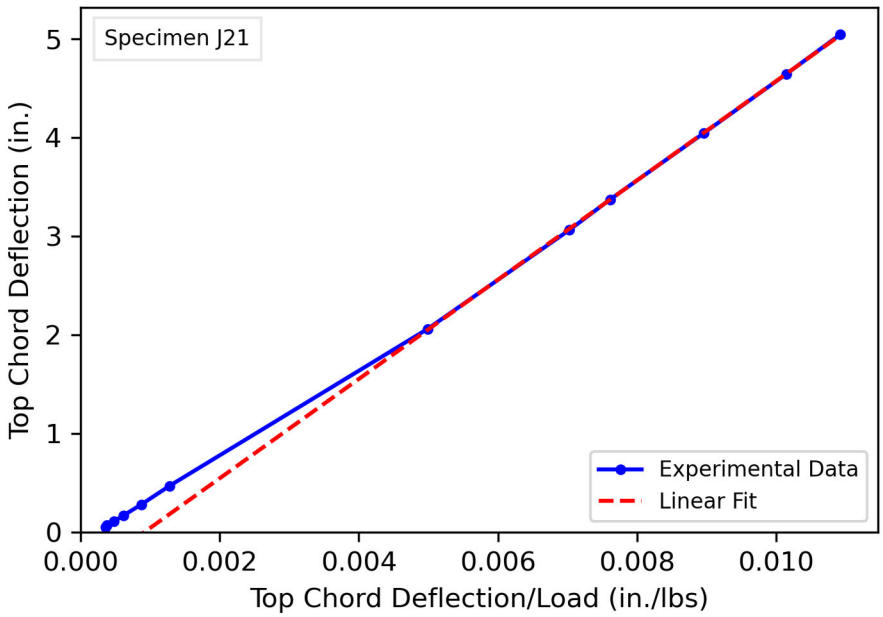

Figure 7: Southwell plot for example joist

4. Results and Discussion

The joists exhibited typical lateral-torsional buckling behavior in the in-plane bending experiments as shown in Fig. 8. At low loads the change in deflection was small as each angle weight was placed on the loading rig. The change in deflection with each angle weight increased with increasing load. Much of the observed deflection occurred with the addition of the last few angle weights. The lateral movement of the top chord was greater than that of the bottom chord resulting in twist of the joist. Deflection was not measured at the ends of the joists, however, based on visual observations, twist at the ends of the joists appeared to be fully restrained and out-of-plane rotation at the ends appeared to be partially restrained.

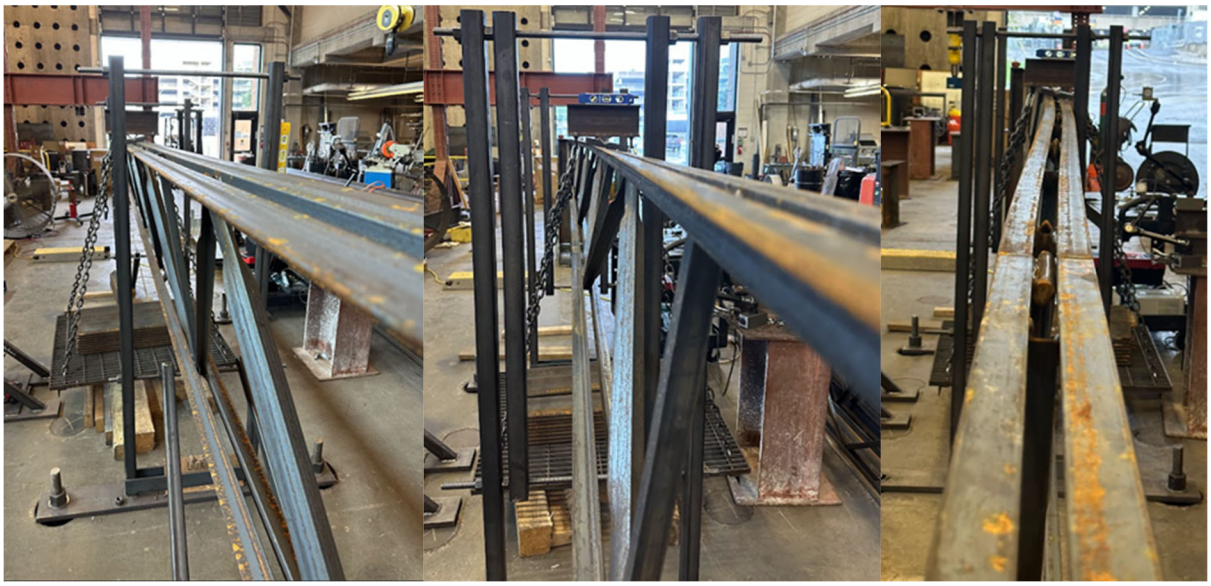

Figure 8: Photographs of deflected joists

Results for each of the joist and connection configurations are listed in Table 4. In all cases, the Southwell buckling load is greater than the load at the deflection limit. The magnitude of deflection for a given applied load depends on the out-of-straightness. A more out-of-straight joist will reach the deflection limit at a lower load. The Southwell buckling load, in effect, corrects for differences in out-of-straightness by extrapolating to the point of infinite deflection. Accordingly, the difference between the Southwell buckling load and the deflection limit load depends on the out-of-straightness.

The average ratio of the Southwell buckling load for the flush frame joists to the Southwell buckling load for the bearing seat joist of the same series is 1.21, 1.83, 1.74, and 1.11 for the J1, J2, J3, and J4 series, respectively. The same average ratio for the load at the deflection limit is 1.18, 1.70, 1.82, and 1.12 for the J1, J2, J3, and J4 series, respectively. In a few cases, the ratio is less than 1.0, indicating that the joist with a flush frame connection was weaker than the joist with a bearing seat connection. However, on average, the joists with flush frame connections supported higher loads than those with bearing seat connections, with the most significant difference observed for the J2 and J3 series joists.

Table 4: Experimental results

Specimen	Southwell Buckling Load (lbs)	Effective Length Factor, *k*	Load at Deflection Limit (lbs)	Effective Length Factor, *k*	Out-of-straightness (in.)
J11	709	0.723	632	0.752	1/8
J12a	861	0.678	754	0.709	1/2
J12b	801	0.694	695	0.728	1/2
J12c	928	0.661	833	0.685	1/2
J12d	801	0.694	719	0.720	3/8
J12e	874	0.674	722	0.719	1/2
J12f	878	0.673	770	0.704	9/16
J13a	882	0.672	785	0.699	5/8
J13b	721	0.719	642	0.748	1/4
J13c	836	0.684	666	0.739	5/8
J13d	866	0.676	798	0.695	1/4
J13e	994	0.646	734	0.715	1
J13f	849	0.681	775	0.702	1/2
J13g	865	0.677	789	0.698	1/4
J13h	882	0.672	762	0.706	1/2
J21	506	0.786	455	0.810	1/4
J22a	917	0.658	720	0.709	9/16
J22b	924	0.657	692	0.717	7/16
J22c	908	0.660	748	0.701	5/8
J22d	996	0.642	766	0.696	11/16
J22e	948	0.652	740	0.703	3/8
J22f	947	0.652	738	0.704	1/2
J23a	913	0.659	830	0.679	1/8
J23b	877	0.668	790	0.689	3/16
J23c	886	0.666	780	0.692	1/4
J23d	922	0.657	750	0.700	1/8
J23e	998	0.641	793	0.689	9/16
J23f	890	0.665	776	0.693	1/4
J23g	930	0.656	846	0.675	1/8
J23h	933	0.655	819	0.682	1/8

Table 4: Experimental results (continued)

Specimen	Southwell Buckling Load (lbs)	Effective Length Factor, *k*	Load at Deflection Limit (lbs)	Effective Length Factor, *k*	Out-of-straightness (in.)
J31	469	0.807	354	0.861	7/16
J32a	720	0.722	544	0.778	3/4
J32b	964	0.663	623	0.751	1 3/4
J32c	761	0.710	626	0.750	1/2
J32d	785	0.704	596	0.760	7/8
J32e	832	0.693	627	0.749	7/8
J32f	823	0.695	589	0.762	1
J33a	804	0.699	658	0.740	1/4
J33b	846	0.689	661	0.739	1/4
J33c	845	0.689	680	0.733	1
J33d	774	0.707	654	0.741	1/4
J33e	875	0.682	723	0.721	1
J33f	763	0.710	636	0.747	7/16
J33g	847	0.689	700	0.727	1
J33h	794	0.702	711	0.724	1/2
J41	735	0.709	493	0.779	2 1/4
J42a	918	0.669	507	0.774	2 3/8
J42b	950	0.663	535	0.765	2 1/4
J42c	881	0.676	477	0.784	2 3/4
J42d	895	0.673	531	0.766	2
J42e	934	0.666	571	0.753	2 3/8
J42f	831	0.687	480	0.783	2 1/4
J43a	840	0.685	588	0.748	1 1/2
J43b	670	0.725	488	0.780	1 1/2
J43c	752	0.705	571	0.753	1 1/2
J43d	720	0.712	545	0.761	1 1/4
J43e	852	0.682	680	0.723	7/8
J43f	717	0.713	573	0.753	1 3/8
J43g	757	0.703	617	0.740	1 1/4
J43h	700	0.717	589	0.748	1 1/8

Fig. 9 shows how the Southwell buckling load varies with connection eccentricity. Note, however, that the girder-side connection plate thickness also varied with connection eccentricity (Table 3). The critical load at 6 in. eccentricity was lower than that for 3 in. eccentricity for most joists. This difference could have been caused by a reduced connection stiffness with the higher eccentricity. The critical load at 9 in. eccentricity was greater than that for 6 in. eccentricity for most joists. The girder-side connection plate was thicker for the connections with 9 in. eccentricity, leading to an apparent increase in stiffness despite the greater eccentricity. The critical load at 12 in. eccentricity was lower than that for 9 in. eccentricity for most joists, continuing the observed trend of decreasing stiffness with increasing eccentricity for a given plate thickness.

Eq. 2a was used to compute the critical load given a distributed load equal to the self-weight, taken as the joist weight divided by the design length from Table 1 for the bearing seat joist of each series. The joist weight divided by the design length was higher for the joists with flush frame connections due to the connection plates at the ends. Extra weight at the ends has minimal impact on buckling behavior. The vertical location of the point load with respect to the shear center, a_e, was computed as $a_e = y_t + y + y_o + 0.5$ in. where y_t is the distance from the top of the top chord to the centroid of the top chord, y is the distance from the centroid of the top chord to the centroid of

the cross section, y_o is the distance from the centroid of the cross section to the shear center, and 0.5 in. is the depth of the knife edge plate.

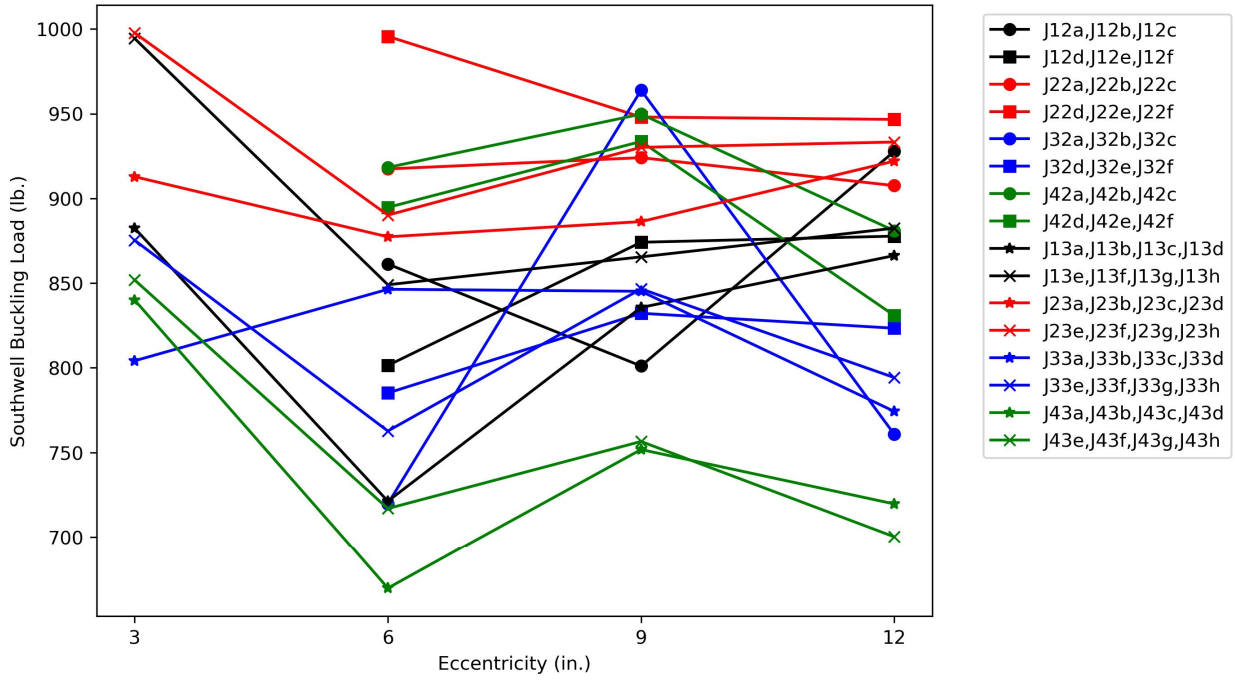

Figure 9: Southwell buckling load vs connection eccentricity

The cross-sectional properties and other parameters used in the Minkoff equation are listed in Table 5. Cross-sectional properties of the chords were computed using the dimensions listed in Table 2 and assuming the angles had the shape of two rectangles, neglecting corner radii.

Table 6 lists the calculated critical load, P, from the Minkoff equation (Eq. 2a) for each series of joists and different values of effective length factor, k. The critical loads with $k = 1.00$, i.e., the value from the original derivation by Minkoff (1975), are less than the experimentally obtained strengths across all joists and connection configurations. The critical loads with $k = 0.85$, i.e., the value specified in the SJI *Specifications* (2020), are less than the experimentally obtained strengths for all joists and connection configurations except the deflection limit load for J31, a joist with a bearing seat connection.

The value of the effective length factor that results in the Minkoff equation giving the same critical load as from the experiment was back-calculated using an iterative approach and is listed for each configuration and both definitions of experimental critical load in Table 4.

The buckling loads of the bearing seat joists are generally lower than those for the flush frame joists, thus their back-calculated effective length factor is higher. Only for the deflection limit load for J31 is the effective length factor greater than 0.85, the value listed in the SJI *Specifications* (2020). The back-calculated effective length factor for J31 is 0.861 for the deflection limit load and 0.807 for the Southwell buckling load. The effective length factor for the bearing seat joists is as low as 0.709 for the Southwell buckling load for J41. These results confirm that the use of $k = 0.85$ is conservative in cases but appropriate overall for bearing seat joists.

Table 5: Parameters used in the Minkoff equation

		Joist Series			
Parameter	**Units**	**J1**	**J2**	**J3**	**J4**
w	lb./in.	0.571	0.712	1.142	1.345
L	in.	384	528	648	720
a_e	in.	7.30	11.97	14.42	16.50
β_x	in.	4.476	7.186	2.168	0
y_o	in.	-0.802	-2.273	-0.097	0
I_y	in.^{4}	1.514	2.535	5.450	8.316
C_w	in.^{6}	104.4	500.9	1126	1946
J	in.^{4}	0.011	0.014	0.064	0.061
y_t	in.	0.432	0.551	0.592	0.703
y	in.	7.17	13.19	13.43	15.30

Table 6: Minkoff equation results

Joist	**Critical Load, *P* (lbs)**		
Series	***k* = 1.00**	***k* = 0.85**	***k* = 0.75**
J1	257	434	636
J2	194	381	596
J3	149	376	625
J4	73.5	315	582

For the flush frame joists, the back-calculated effective length factor ranges from 0.641 for the Southwell buckling load for J23e to 0.784 for the deflection limit load for J42c. Average values for the effective length factor range from 0.687 to 0.771 for the deflection limit load and from 0.654 to 0.705 for the Southwell buckling load. Based on these results, a value of $k = 0.75$ appears to be appropriate for design of the erection bridging for flush frame joists. Note, however, that the critical load was shown to vary with connection eccentricity and girder connection plate thickness. These values of k should not be used for thinner plates or larger eccentricities than those tested in this study where the flexibility of the connection could be greater and the critical buckling load lower.

The back-calculated effective length factor results also help shed light on the strength results. The increase in strength for a flush frame joist in comparison to a bearing seat joist was less for the J1 and J4 series joists than it was for the J2 and J3 series joists. The effective length factors for the flush frame joists are relatively consistent. The effective length factors for the bearing seat joists are less consistent. Based on the Southwell buckling load, $k = 0.723$ and 0.709 for joists J11 and J41, respectively; and $k = 0.786$ and 0.807 for joists J21 and J31, respectively. These results indicate that the reason that there was less difference in strength between the bearing seat joists and the flush frame joist for the J1 and J4 series joists is because the bearing seat joists were relatively strong and not because the flush frame joists were relatively weak. Joists J11, J21, and J31 all had similar bearing seat details, but joist J11 was smaller and thus the relative restraint provided by the bearing seat could have been higher. Joist J41 was an LH series joist with a larger bearing seat than the other joists (which were K series joists) and thus also could have had greater end restraint.

To illustrate the impact of different effective length factors, the length at which erection bridging is required was computed for the different joists and different values of k. The length was computed

as the length, L, at which P from Eq. 2a equals 300 lbs. The resulting values are listed in Table 7. Changing from $k = 0.85$ to $k = 0.75$ results in an approximately 11% increase in the length at which erection bridging is required for the joists investigated.

Table 7: Calculated length at which erection bridging is required

Joist Series	Length (ft) when P = 300 lbs		
	k = 1.00	k = 0.85	k = 0.75
J1	30.7	35.6	39.9
J2	40.2	46.5	52.0
J3	49.0	56.2	62.3
J4	52.8	60.4	67.0

5. Conclusions and Recommendations

Accurately evaluating the potential for lateral-torsional buckling is critical for safe and efficient erection of open web steel joists. If a joist cannot support its own weight and the weight of an erector, bridging must be installed before the hoisting cables are released. The potential for lateral-torsional buckling of joists is evaluated in practice using the Minkoff equation which was derived and validated for joists with typical bearing seat connections. Flush frame connections for joists have been recently developed and are particularly attractive in composite floor systems controlled by vibrations. Flush frame connections also provide greater connection stiffness than bearing seat connections. However, the greater stiffness provided by flush frame connections is not yet recognized in the design of erection bridging.

This study investigated the erection stability of joists with flush frame connections with physical experiments to better understand the impact of the increased connection stiffness and develop recommendations for design. Bending tests of 60 different joist and connection configurations without bridging were performed to determine the critical load. The critical load of joists with flush frame connections was almost always greater than that for joists with bearing seat connections. The Minkoff equation with an effective length factor of $k = 0.75$ was found to provide a generally conservative approximation of the strength of joists with flush frame connections.

Based on these results, a modification to the SJI *Specifications* to allow the use of $k = 0.75$ in the Minkoff equation for joists with flush frame connections is recommended. Noting that the stiffness of flush frame connections depends on connection eccentricity and plate thickness, without further research, the recommended effective length factor should not be used for connections less stiff than those tested in this study. Specifically, the recommended effective length factor should be used only when the girder connection plate thickness is greater than or equal to 1/4 in. when the eccentricity is less than or equal to 6 in. and 1/2 in. when the eccentricity is between 6 and 12 in.

Use of the recommended effective length factor will allow more joists to be erected without erection bridging and without compromising safety. For ease of use, limiting lengths for all standard SJI joists should be calculated and provided to engineers. Additional research on the erection stability of other types of joists for which the Minkoff equation does not directly apply, such as pitched joists, is also recommended.

Acknowledgments

This research was funded by the Steel Joist Institute (SJI). The joists were manufactured and delivered to the University of Tennessee, Knoxville campus by Vulcraft-Alabama. The support of both SJI and Vulcraft is gratefully acknowledged. The authors thank Pratik Poudel, Larry Roberts, Andy Baker, and Caroline Dykes for their support performing the physical experiments.

References

Davis, B., and Murray, T. M. (2022). "Vulcraft Vibration Research Composite Joists with Flush Framed Connections 1785 Columbus Avenue, Boston, MA."

Galambos, T. V. (1993). "Bracing of Trussed Beams." *Is Your Structure Suitably Braced?*, Structural Stability Research Council, Milwaukee, Wisconsin.

Mandal, P., and Calladine, C. R. (2002). "Lateral-torsional buckling of beams and the Southwell plot." *International Journal of Mechanical Sciences*, 44(12), 2557–2571.

Minkoff, R. M. (1975). "Stability of Joists During Erection." M.S. Thesis, Washington University, St. Louis, Missouri.

Moore, J. A., and Denavit, M. D. (2024). *Diagonal Erection Bridging for Open Web Steel Joists with Flush Frame Connections*. Report Submitted to the Steel Joist Institute, University of Tennessee, Knoxville, Knoxville, Tennessee.

Murray, T. M., and Davis, B. (2020). "Vibration of Vulcraft Steel Joists with Flush Framed and Flush Bearing Seat Connections."

SJI. (2020). *Standard Specifications for K-Series, LH-Series, and DLH-Series Open Web Steel Joists, and for Joist Girders*. ANSI/SJI 100-2020, Steel Joist Institute, Florence, South Carolina.

Slein, R., Buth, J. S., Latif, W., Kamath, A. M., Alshannaq, A. A., Sherman, R. J., Scott, D. W., and White, D. W. (2020). "Large-scale experimental lateral-torsional buckling tests of welded I-section members." *Proceedings of the Annual Stability Conference*, Structural Stability Research Council, Atlanta, Georgia.

Vulcraft. (2023). "Joist Flush Frame Connections." <https://vulcraft.com/Products/FlushFrameConnections>.

Ziemian, R. D., Schwarz, J. E., Emerson, M. R., and Potts, D. R. (2004). "Stability of Unbraced Steel Joists Subject to Min-Span Loading." *Proceedings of the Annual Stability Conference, Structural Stability Research Council*, Long Beach, California.